Eur. Phys. J. B **58**, 353–360 (2007)
DOI: 10.1140/epjb/e2007-00244-x

THE EUROPEAN PHYSICAL JOURNAL B

Propagation properties of elastic waves in semi-infinite phononic crystals and related waveguides

Y.W. Yao[1,2,a], F.G. Wu[3], Z.L. Hou[1], and Y.Y. Liu[1]

[1] Department of Physics, South China University of Technology, Guangzhou 510640, P.R. China
[2] Department of Applied Physics, Guangdong University of Technology, Guangzhou 510090, P.R. China
[3] Experiment Center and Department of Applied Physics, Guangdong University of Technology, Guangzhou 510090, P.R. China

Received 28 October 2006 / Received in final form 22 July 2007
Published online 22 September 2007 –

Abstract. The transmission and reflection coefficients of two-dimensional semi-infinite solid-solid phononic crystal systems and fluid-fluid phononic waveguide structures have been investigated. The numerical results show that the transmission spectra for longitudinally and transversally polarized incident waves are different, and the spectra of the transmission and reflection coefficients of the semi-infinite system agree well with the band structure. The numerical results show that when a guided wave incident, localized modes are excited, and different polarities have different coupling efficiencies with the incident guided wave. At the same time, far from the cutoff frequency, the guided wave couples out of semi-infinite waveguide highly efficiently.

PACS. 43.20.+g General linear acoustics – 43.40.+s Structural acoustics and vibration – 46.40.cd Mechanical wave propagation (including diffraction, scattering, and dispersion)

1 Introduction

The study of acoustic or elastic wave propagation in one-dimensional periodic composite materials [1–3] is an old problem which originates from the description of the propagation of seismic shocks through the Earth's crust. In recent years, inspired by the success of studies of photonic crystals, physicists extended their study from one-dimensional to two and three dimensional periodic composite materials [4–20]. Periodic composite material is also called phononic band gap material or phononic crystal. The key aim behind the proposal of phononic crystals is the possibility of modifying the propagation of acoustic or elastic waves by creating phononic band gaps in the band structure of the synthetic periodic structures, by analogy with the photonic band gap in periodic dielectric structures and the electronic band gaps in semiconductor crystals. Theories show that the large contrast between the elastic parameters (the mass density and the velocity) of the scattering and the host material is a necessary condition for the existence of phononic band gaps. Besides the band gap, the transmission (reflection) spectrum also plays an important role in revealing the physical property of these composite materials. For example, Khelif et al. [17,18] used the FDTD method to calculate the transmission coefficient and found that the transmission of elastic waves through the waveguide can be significantly altered by incorporating a cavity inside or at the side of the guide. A different position of the cavity will give different effects on the transmission behavior. They also observe that the bend phononic waveguides have a low loss transmission different from conventional waveguides. Zhang et al. [21] have demonstrated that negative refraction of acoustic waves in the 2D phononic crystal exists in a manner similar to that of photonic crystals from the transmission spectra. Hou et al. [22,23] have evaluated the effective velocity of the phononic crystal from the oscillation period of the transmission and reflection spectra.

The propagation of elastic or acoustic waves in a one-dimensional semi-infinite periodic composite material and two-dimensional finite phononic crystals have been extensively investigated as mentioned above. But until now, to the best of our knowledge, there are no articles devoted to the study of elastic (acoustic) wave propagation in semi-infinite two-dimensional phononic crystals and related waveguide structures with their surfaces parallelling to the axes of the rods. Although there are a few studies of the semi-infinite two-dimensional phononic crystal [24,25], they focus their attention on the surface wave band structure, and the surface of these system is perpendicular to the axes of the rods. A simple case in the present paper is a plane wave with frequency f and wave vector k_0 normally incidents from the left (homogenous material) to the semi-infinite phononic crystal along the y axis, the configuration of which is schematically depicted in Figure 1a.

[a] e-mail: yaoyw@scut.edu.cn

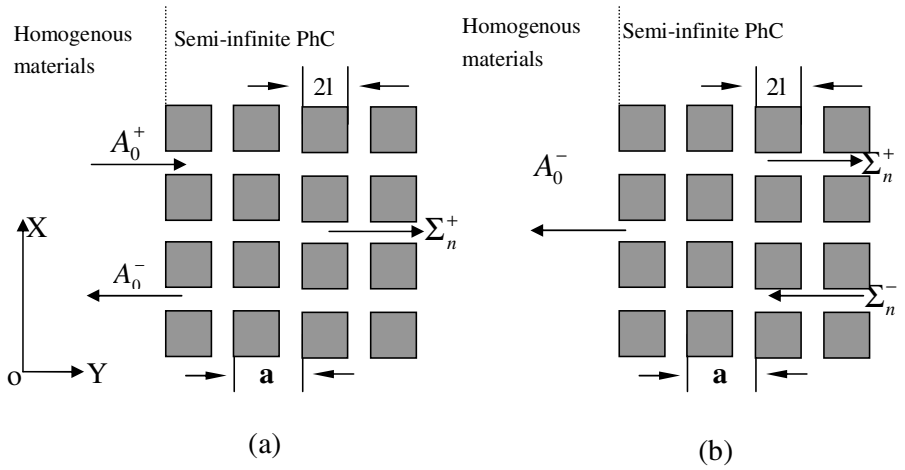

Fig. 1. (a) An external elastic wave propagating from left to right is scattered by a semi-infinite phononic crystal which consists of square lead rods embedded in an epoxy matrix. (b) The elastic wave propagates from deep inside the semi-infinite phononic crystal into the host material.

Evidently, the semi-infinite model is different from the finite-size phononic crystal, due to the fact that it has only one interface, whilst the finite-size model has two between the homogenous host material and the phononic crystal under study. In this case, we would expect very different propagation properties, and the system is worthy of investigation. A one-dimensional transfer matrix has been used to investigate the transverse and sagittal elastic waves in the one-dimensional semi-infinite system [2,3], but it is not possible to solve the two-dimensional system in the way because the material is inhomogenous along the direction perpendicular to the propagation direction in the two-dimensional phononic crystal. For two-dimensional semi-infinite systems, all the previous studies have used the plane wave expansion method. It is well-known that this method is effective for calculating the band structure, but it is seldom used to calculate the transmission and reflection coefficients. Recently, we have developed a new numerical method, improved eigen-mode matching theory (IEMMT) based on eigen-mode matching theory (EMMT) [23,26,27]. Practice shows that it is not only a very efficient approach to calculate the transmission and reflection coefficients of finite size phononic crystals, but can also calculate the band structure of the infinite phononic crystal. In the present article, we combine the IEMMT method with the Bloch mode expansion method, which has been successfully used in semi-infinite photonic crystals [28–31], to investigate the elastic wave propagation properties of the two-dimensional semi-infinite phononic crystals and related waveguide structures.

This paper is organized as follows. In Section 2, we briefly present the main calculation idea of the Bloch mode expansion method based on the IEMMT method for elastic (acoustic) wave propagation in the two-dimensional semi-infinite phononic crystal and sandwiched phononic crystal waveguide structures. The numerical results and discussion for the two-dimensional semi-infinite phononic crystal and sandwiched phononic crystal waveguide structures are presented in Sections 3 and 4, respectively. In Section 5, A brief summary is given.

2 The formulism for wave propagation in semi-infinite phononic crystals and related waveguide structures

Elastic wave propagation in elastic media can be described by

$$\rho \frac{\partial^2 U_i}{\partial t^2} = T_{ij,i} \tag{1}$$

$$T_{ij} = C_{ijkl} U_{k,l}, \tag{2}$$

where $i, j, k, l = 1, 2, 3$, respectively, T_{ij} is the stress tensor component, U_i is the elastic displacement vector, ρ is the mass density and c_{ijkl} is the elastic stiffness.

In the present article, since only elastic waves in the XY plane are considered, and the elastic materials are isotropic, equations (1) and (2) can be rewritten as:

$$-\rho\omega^2 U_1 = (C_{11}U_{1,1} + C_{12}U_{2,2})_{,1} + T_{21,2}, \tag{3}$$

$$-\rho\omega^2 U_2 = (C_{44}U_{1,2} + C_{44}U_{2,1})_{,1} + T_{22,2}, \tag{4}$$

$$T_{21} = C_{44}U_{1,2} + C_{44}U_{2,1}, \tag{5}$$

$$T_{22} = C_{12}U_{1,1} + C_{11}U_{2,2}, \tag{6}$$

where $C_{11} = C_{12} + 2C_{44}$.

Due to the periodic boundary condition along the x-direction, the plane-wave expansion of equations (3–6) along the x-direction reads

$$\sum_{G'}[-C_{11G-G'}(k_x+G)(k_x+G') + \omega^2\rho_{G-G'}]U_{1K_x+G'} = \beta_y[\sum_{G'} C_{12}(k_x+G)U_{2K_x+G'} - iT_{21K_x+G}], \tag{7}$$

$$\sum_{G'}[-C_{44G-G'}(k_x+G)(k_x+G')+\omega^2\rho_{G-G'}]U_{2K_x+G'}=$$
$$\beta_y[\sum_{G'}C_{44}(k_x+G)U_{1K_x+G'}-iT_{22K_x+G}], \quad (8)$$

$$-\sum_{G'}[C_{44G-G'}(k_x+G)]U_{2K_x+G'}-iT_{21K_x+G}=$$
$$\beta_y[\sum_{G'}C_{44G-G'}U_{1K_x+G'}], \quad (9)$$

$$-\sum_{G'}[C_{12G-G'}(k_x+G)]U_{1K_x+G'}-iT_{22K_x+G}=$$
$$\beta_y[\sum_{G'}C_{11G-G'}U_{2K_x+G'}]. \quad (10)$$

The above four equations construct the eigen-equations for β_y. After the eigenvalues and the eigenvectors are solved from the eigen-equations, the wave function can be written as the follows [23,26].

$$\begin{pmatrix}\mathbf{U}_2\\ \mathbf{U}_1\\ -\mathbf{iT}_{22}\\ -\mathbf{iT}_{21}\end{pmatrix}=\sum_{n=1}^{N}e^{j\alpha_n x}\left(\sum_{r=1}^{2N}A_{rL}e^{i\beta_{rL}y}\begin{pmatrix}\mathbf{u}_{nL}^r\\ \mathbf{t}_{2nL}^r\end{pmatrix}+\sum_{r=1}^{2N}A_{rR}e^{i\beta_{rR}y}\begin{pmatrix}\mathbf{u}_{nR}^r\\ \mathbf{t}_{2nR}^r\end{pmatrix}\right), \quad (11)$$

where $[\mathbf{u}_n^r,\mathbf{t}_n^r]^t$ is the eigenvector associated with eigenvalue β_r, and the boundary condition gives

$$\begin{pmatrix}\dot{\mathbf{U}}^{+i}\\ \mathbf{iT}_2^{+i}\end{pmatrix}=\begin{pmatrix}\dot{\mathbf{U}}^{-i+1}\\ \mathbf{iT}_2^{-i+1}\end{pmatrix} \quad (12)$$

where $\mathbf{U}=(U_1,U_2)^t,\mathbf{iT}_2=(iT_{21},iT_{22})^t$, and superscript $+(-)$ i denotes the right(left) boundary of the ith layer.

With the help of the boundary condition, we can construct the S-matrix for the unit cell [27]. After the S-matrix of unit cell is obtained, there exists the relation

$$\begin{pmatrix}A_i^+\\ A_i^-\end{pmatrix}=\begin{pmatrix}I & -S_{12}\\ 0 & -S_{22}\end{pmatrix}^{-1}\begin{pmatrix}S_{11} & 0\\ S_{21} & -I\end{pmatrix}\begin{pmatrix}A_{i-1}^+\\ A_{i-1}^-\end{pmatrix}=T\begin{pmatrix}A_{i-1}^+\\ A_{i-1}^-\end{pmatrix}. \quad (13)$$

Using Bloch theorem, the relationship between the elastic fields of both sides of the unit cell is

$$\begin{pmatrix}A_i^+\\ A_i^-\end{pmatrix}=e^{i\mathbf{k_y}\mathbf{R_y}}\begin{pmatrix}A_{i-1}^+\\ A_{i-1}^-\end{pmatrix}, \quad (14)$$

where $\mathbf{k}$ is the Bloch wave vector and $\mathbf{R}$ is the primitive lattice vector of the phononic crystal. From equations (13) and (14), we have

$$T\begin{pmatrix}A_{i-1}^+\\ A_{i-1}^-\end{pmatrix}=e^{i\mathbf{k_y}\mathbf{R_y}}\begin{pmatrix}A_{i-1}^+\\ A_{i-1}^-\end{pmatrix}, \quad (15)$$

Equation (15) can be re-written as

$$TE=E\Lambda, \quad (16)$$

where Λ is a diagonal matrix composed of all eigenvalues $(\lambda_i,i=1,2...N)$, N is the dimension of T. E is a $N\times N$ matrix with its ith column being the eigenvector of T corresponding to the eigenvalue λ_i. Furthermore, T can be expressed as $T=E\Lambda E^{-1}$, putting T into the eigen-equation

$$T\begin{pmatrix}A^+\\ A^-\end{pmatrix}=\lambda\begin{pmatrix}A^+\\ A^-\end{pmatrix}, \quad (17)$$

and after a simple deduction, we have

$$\Lambda\Sigma=\lambda\Sigma, \quad (18)$$

where $\Sigma=E^{-1}(A^+,A^-)^{\mathrm{T}}$, here "T" denotes the matrix transposition, A^+ and A^- are the amplitudes of the elastic field in the layer under study. For a general column vector $\Sigma=(\sigma_i,i=1,...,N)$, in which element σ_i denotes an eigen-mode of the transfer matrix T. This equation $\Sigma=E^{-1}(A^+,A^-)^{\mathrm{T}}$ is very important in the latter calculation, because it gives the transformation relationship between the eigen-mode of the original plane-wave basis and that of the new eigen-state basis. In the new eigen-state basis, we needs separate the original eigen-mode into either positive eigen-mode or negative eigen-mode according to the corresponding eigenvalue. Similar to the literatures [28,29], when the elastic wave propagates from the left (host material) to the right (semi-infinite phononic crystal), we have

$$E^{-1}\begin{pmatrix}A_0^+\\ A_0^-\end{pmatrix}=\begin{pmatrix}\Sigma_0^+\\ \Sigma_0^-\end{pmatrix}=\begin{pmatrix}\Sigma_0^+\\ 0\end{pmatrix}, \quad (19)$$

therefor:

$$A_0^+=E_{11}\Sigma_0^+,A_0^-=E_{21}\Sigma_0^+. \quad (20)$$

From equation (20), we obtain

$$\Sigma_0^+=E_{11}^{-1}A_0^+. \quad (21)$$

In the case of the elastic wave propagating from the left (host material) to the right (semi-infinite phononic crystal), A_0^+ is a known incident value. So, the reflection field in the plane wave basis can be written as

$$A_0^-=E_{21}E_{11}^{-1}A_0^+, \quad (22)$$

and the transmission field reads

$$A_n^+=E_{11}\Sigma_n^+,A_n^-=E_{21}\Sigma_n^+, \quad (23)$$

where Σ_n^+ can be obtained from the equation

$$\Sigma_n^+=\Lambda_+^n\Sigma_0^+,\Sigma_n^-=\Lambda_-^n\Sigma_0^-. \quad (24)$$

Because only the Bloch mode with $|\lambda|=1$ (propagation mode) survives when the elastic wave propagates far from the interface between the host material and the phononic crystal, Σ_n^+ must have the form as: $\Sigma_n^+=[0,...,0,(\lambda_j)^{-1}(E_{11}^{-1}A_0^+)_j,0,...,0]$, where

$\lambda_j = \exp(i\mathbf{k_y}\mathbf{R_y})$. In Section 3, we will use the above theory to perform the numerical calculation of the semi-infinite phononic crystal under study.

When the elastic wave propagates from deep inside the phononic crystal to the host material shown in Figure 1b. The transmission and reflection parameters can be obtained as follows. From equation

$$E\begin{pmatrix}\Sigma_0^+\\ \Sigma_0^-\end{pmatrix} = \begin{pmatrix}0\\ A_0^-\end{pmatrix}, \tag{25}$$

where

$$\Sigma_0^- = (\Lambda_-)^{-n}\Sigma_n^- \tag{26}$$

we get the the transmission field

$$A_0^- = Q_{22}^{-1}\Sigma_0^-, \tag{27}$$

and finally the reflection field

$$\Sigma_0^+ = Q_{12}A_0^-, \tag{28}$$

$$\Sigma_n^+ = (\Lambda_+)^n\Sigma_0^+, \tag{29}$$

where $Q = E^{-1}$. Once Σ_n^+ has been calculated, the reflection field in plane-wave expansion form can be given by equation (23). Using the above formalism, we can also calculate the transmission and reflection coefficient of the inverse process.

In the above, we consider the elastic or acoustic wave scattering by a simple semi-infinite phononic crystal structure. Now, we consider a more complex system shown in Figure 2. The central sandwiched structure is surrounded by two semi-infinite phononic crystal waveguide structures, the two semi-infinite waveguide structures have the same lattice. In this case, using the IMMET method combined with a super-cell approach, we reach the equation:

$$\begin{pmatrix}A_{2,0}^+\\ A_{1,0}^-\end{pmatrix} = S_{PC2}\begin{pmatrix}A_{1,0}^+\\ A_{2,0}^-\end{pmatrix}, \tag{30}$$

where S_{PC2} is the S-matrix of the sandwiched part in Figure 2. From equation (19), we have

$$A_{2,0}^+ = S_2^{11}\Sigma^+, A_{2,0}^- = S_2^{21}\Sigma^+ \tag{31}$$

and

$$A_{1,0}^+ = S_1^{11}\Pi^+ + S_1^{12}\Pi^-, A_{1,0}^- = S_1^{21}\Pi^+ + S_1^{22}\Pi^-. \tag{32}$$

Putting equations (31) and (32) into equation (30), we obtain

$$\begin{pmatrix}S_2^{11} - S_{PC2}^{12}S_2^{21} & -S_{PC2}^{11}S_1^{12}\\ -S_{PC2}^{22}S_2^{21} & S_1^{22} - S_{PC2}^{21}S_1^{12}\end{pmatrix}\begin{pmatrix}\Sigma_0^+\\ \Pi_0^-\end{pmatrix} = \begin{pmatrix}S_{PC2}^{11}S_1^{11}\Pi_0^+\\ (S_{PC2}^{21}S_1^{11} - S_1^{21})\Pi_0^+\end{pmatrix}. \tag{33}$$

We can determine the Σ_0^+ and Π_0^- from the above equation since there exists a relationship $\Pi_0^+ = (\Lambda_+)^{-n}\Pi_n^+$, where Π_n^+ is a Bloch mode from well within the PC1 waveguide. Based on equation (19), equation (33) and the relationship between Π_n^+ and Π_0^+, we can calculate the transmission and the reflection coefficients of the system shown in Figure 2 and other complex sandwiched semi-infinite waveguide structures.

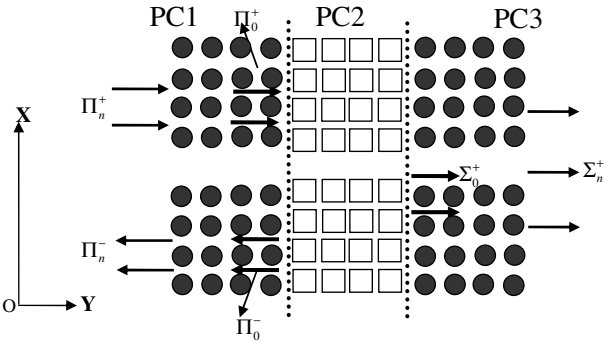

Fig. 2. The sandwiched guided structure, $PC2$ is the central sandwiched party, $PC1$ and $PC3$ are two semi-infinite phononic waveguides.

3 Numerical results for wave transmission and reflection in simple semi-infinite phononic crystal structures

Based on the calculation method developed above, the first system to be investigated is a semi-infinite solid-solid phononic crystal. In the system, the elastic wave properties is more complicated than that of the photonic crystal because of the coexistence of longitudinal and transversal modes. In the studied solid-solid phononic crystal system, the embedded material is chosen to be elastic isotropic rectangular lead rods with parameters $\rho = 11.40 \times 10^3$ kg/m^3, $C_t = 860$ m/s, $C_l = 2160$ m/s, the host material is epoxy with $\rho = 1.180 \times 10^3$ kg/m^3, $C_t = 1157$ m/s, $C_l = 2535$ m/s, and the filling fraction is 0.16 ($l/a = 0.2$). By using a 21 plane wave basis and a frequency step of $0.0005(2\pi C_t/a)$, we calculate the band structure of the two-dimensional infinite phononic crystal along the [10] direction, as shown in Figure 3b. Next, under the assumption that a longitudinally polarized plane wave is normally incident on the semi-infinite phononic crystal along the [10] direction, we calculate the corresponding transmission and reflection spectra and display the numerical results in Figure 3c, where the solid lines show the transmission coefficient and hollow dot lines show the reflection coefficient. Furthermore, when the incident wave is the transversally polarized elastic wave, its transmission and reflection coefficients within the same system are presented in Figure 3a. It is obvious that the curves exhibit smoothly varying behavior and there is no strong oscillations. These phenomena have been well understood in the context of photonic crystals, and more generally optics. The transmittance or reflection oscillation which is evident in a finite structure is the Fabry-Perot resonances caused by the reflections that occur at the rear interface of the finite structure. In a semi-infinite structure, the removal of the back interface eliminates the resonances. Comparing Figure 3a with Figure 3c, we find that the transmission spectra have different propagation behavior when the incident wave is different, for example, in the frequency range between 0 to $1.0(2\pi c_t/a)$, the transmission spectra of the transversal incident wave have two band gaps, but for the longitudinal incident wave there is

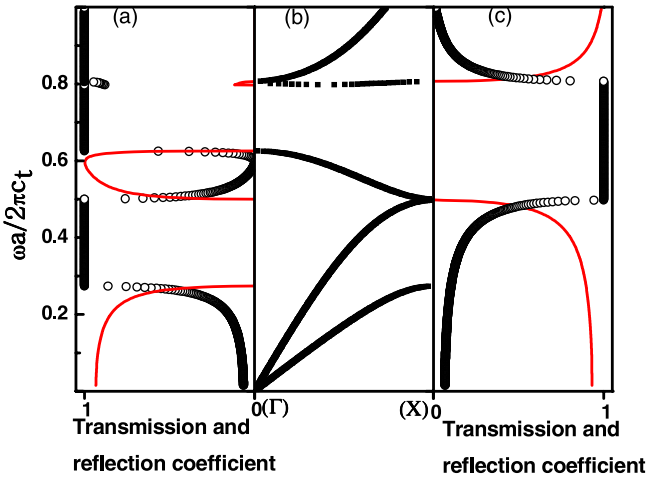

Fig. 3. (a) The transmission and reflection spectra of the semi-infinite solid-solid PhC for a transversal incident wave, where the solid lines show the transmission coefficient and hollow dotted lines are for the reflection coefficient. (b) The band structure of the solid-solid PhC the along [10] direction. (c) The transmission and reflection spectra for a longitudinal elastic incident wave.

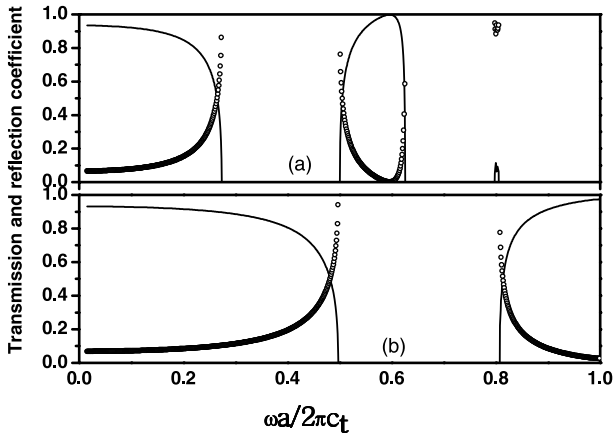

Fig. 4. The transmission and reflection spectra of the Bloch wave propagating from deep inside the semi-infinite phononic crystal into the host material as shown in Figure 1b. (a) For a transversal elastic wave. (b) For a longitudinal elastic wave, where the solid lines show the transmission coefficient and hollow dot lines show the reflection coefficient.

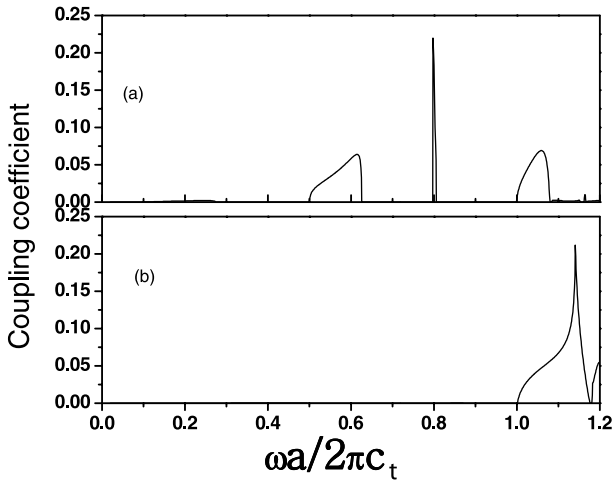

Fig. 5. Different between the transmission coefficient of the excited wave different and the incident wave, here the incident wave is (a) a transverse wave, (b) a longitudinal wave.

only one gap. On the other hand, the transmission spectra of both the longitudinal and transversal incident cases also have some common character. For frequencies below the first band gap, the transmission coefficient shows a very simple monotonous decaying behavior, and the reflection coefficient is increases monotonously. When the frequency of the incident wave lies within the band gap, the transmission coefficient is exactly zero and the reflection coefficient is precisely unity. From the spectra, we also find that the transmission and reflection spectra agree with the band structure very well, i.e., the common gap in the transmission coefficient for both of the longitudinal and transversal incident cases is exactly the gap of the band structure.

Next, we consider an inverse process, i.e., a Bloch wave propagates from deep inside the phononic crystal into the homogenous part along the [10] direction. This process has been shown in Figure 1b, and the formula to calculate the transmission and reflection coefficient has been given in Section 2. For this case, we emphasize again that there only one Bloch mode exists deep inside the semi-infinite phononic crystal. The numerical results of the transmission and reflection coefficients are plotted in Figure 4. Panel (a) of Figure 4 is for the transversally polarized wave, and panel (b) is for the longitudinally polarized wave. The solid line indicates the transmission spectra, and the hollow dot line indicates the reflection spectra. Because no Bloch modes exist in the band gap, all the transmission and reflection coefficients are absent in that region. Comparing Figure 3 with Figure 4, it can be seen that the spectral curves for the longitudinal wave and transversal waves are respectively identical to each other. The reason for this is stated as follows. First, just as photonic crystal [28], this phononic crystal system also has time-reversal symmetry. So, there exists an identity of the transmission coefficient in the two inverse wave propagation processes. Secondly, in our calculation, only zero-order Bragg waves exist in the homogenous material region, so that when the elastic wave normally incidents only one Bloch mode can be excited in the phononic crystal. These two points guarantee that both the original and inverse processes are symmetric when time is reversed.

It is general that the eigenmodes of the phononic crystal are always hybrid in the xy-plane. When the longitudinal or transverse wave is incident on the semi-infinite phononic crystal, both longitudinal and transverse waves will be excited. In order to show how the excited waves differ from the incident wave, we switch off all modes the same as incident wave by making their amplitude equal to zero. The numerical results of the coupling are shown in Figure 5. Panel (a) shows the transmission coefficient of the longitudinal waves when the transverse wave is incident, and panel (b) shows the coupling of the transverse

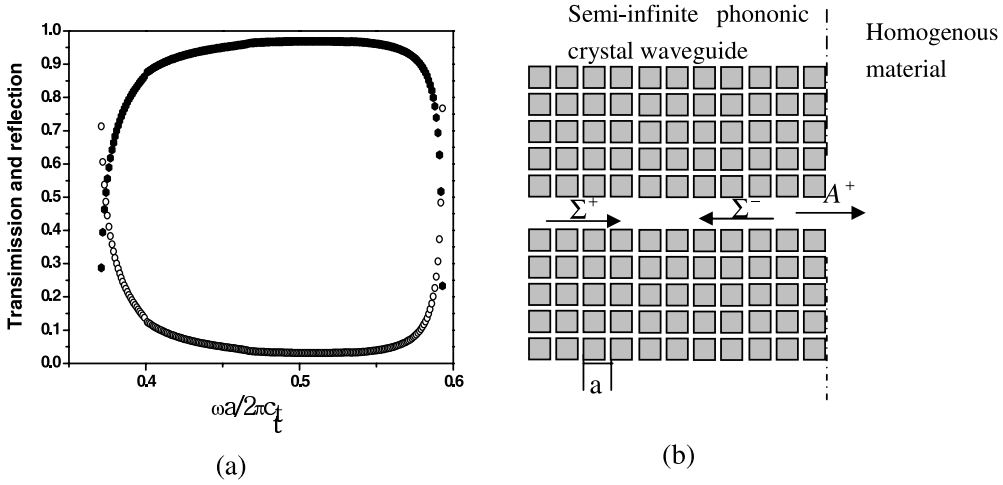

Fig. 6. The transmission and reflection coefficients of the guide wave coupling out of the semi-infinite phononic waveguide.

wave to the incident longitudinal wave. From the figure, it is found that when the normal incident wave is longitudinal wave, there is no transverse mode coupling to the external wave in the low frequency region, and when the incident wave is transverse, the longitudinal wave is excited in some low frequency region, but not all low frequency region. This special situation arises due to the normal incident ($k_{||} = 0$), the details of which have been given in reference [7]. Because there only exists weak coupling when the wave is normal incident, in the low frequency region, the longitudinal and transverse vibrations are almost decoupled from each other along the Gamma-X direction of the Brillouin zone in the discussion of Figures 3 and 4.

4 Wave transmission and reflection in semi-infinite phononic crystal waveguide structures

In the last section, we use the IMMET method combined with the Bloch mode expansion method to study elastic wave propagation in the simple semi-infinite two dimensional solid-solid phononic crystal. In this section, three complex systems will be investigated. The first system to be investigated is shown in Figure 6b. The waveguide is created by removing a single row of square rods along the [10] direction from a semi-infinite fluid-fluid phononic crystal. In the system, the scatterer is an elastic isotropic square water rod with parameters $\rho = 1.0 \times 10^3$ kg/m^3, $C_l = 1480$ m/s, which forms a square lattice, embedded in the host mercury with $\rho = 13.50 \times 10^3$ kg/m^3, $C_l = 1450$ m/s with filling fraction 0.36 ($l/a = 0.3$), where a is the lattice constant, these parameters will be unchanged in the following section of the paper. In the numerical calculation 81 plane waves are adopted and 15 unit cells are included in a super-cell. The process of the guided wave coupling out of the waveguide is also shown in Figure 6b, the guided mode Σ^+ start first in the depth of the waveguide, then it impinges on the waveguide exit, some part of the guided mode reflects back and exists as the negative propagation guide mode in the waveguide, the other part of the positive guide mode will couple out of the waveguide in the form of A^+. The transmission and reflection coefficient of the guided mode are shown in Figure 6a, the result shows that the transmission coefficient almost monotonously increases until the frequency of the guided mode exceeds the normalized frequency ($0.551\omega a/2\pi c_t$), and the transmission coefficient is not very high when the frequency is near the cutoff frequency. This means that the coupling efficiency varies with the frequency of the incident guided mode, and far from the cutoff frequency, the guided wave couples out of the waveguide with very high efficiency.

The second investigated system is shown in the right panel of Figure 7a, which is a two-dimensional phononic cavity between two identical semi-infinite phononic waveguides. The two-dimensional phononic cavity is formed by placing two identical square rods into the waveguide and keeping a vacant region between the rods. Because the rods placed into the waveguide are the same as the others in the phononic waveguide structure, each wall of the cavity is one unit-cell thick and the width of the cavity is one unit-cell wide. Using the formula given in Section 2, the numerical results are shown in the left panel of Figure 7a. From the figure, there is only one resonant peak at the normalized frequency $\omega_0 = 0.514\ \omega\ a/2\pi c_t$, although the frequency of the incident guided mode ranges from ($0.360\omega a/2\pi c_t$) to ($0.595\omega a/2\pi c_t$). The resonant frequency is very close to the frequency of the cavity mode, which is calculated by the plane wave method with 961 plane waves and a 15×15 super cell. This agreement tells us that the transmission peak is induced by the cavity mode coupling with the incident guided wave. Now, we change the geometrical parameters of the center cavity; the width of the cavity becomes two unit-cells and the thickness of the wall is still one unit-cell thick. The changed structure is shown in the right panel of Figure 7b, the transmission coefficient of the structure is shown in the

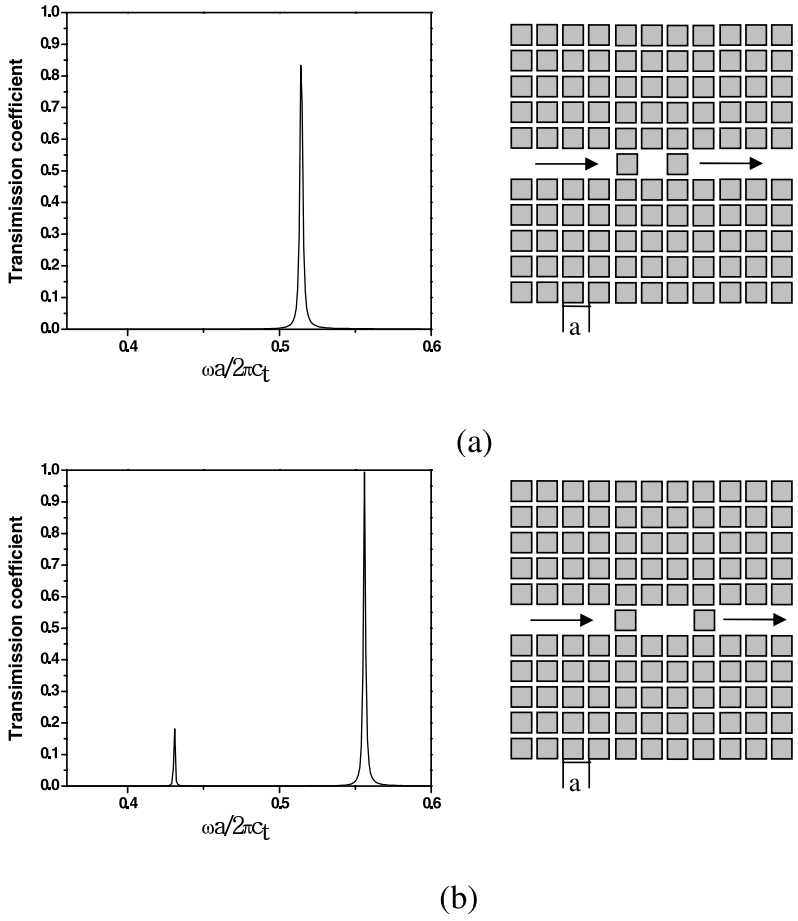

Fig. 7. The transmission and reflection coefficient of the guide wave propagation in the sandwiched phononic waveguide structures, (a) the width of cavity is one unit-cell wide, (b) the width of cavity is two unit-cells wide.

left panel of Figure 7b. The result shows that there exists two resonant peaks located at the frequencies $\omega_1 = 0.431$ $\omega\ a/2\pi c_t$ and $\omega_2 = 0.556\ \omega\ a/2\pi c_t$, respectively. The resonant peaks have different amplitudes. The peak corresponding to the resonant frequency ω_1 is 0.181, and the other is 0.994. It has been demonstrated that when the width of the cavity become two unit-cells wide, the degenerate mode will split into two modes, and the two modes have different polarity [32]. When the guided wave is incident, the localized mode will be excited, and the different amplitude resonant peaks mean that the different polarity has a different coupling efficiency with the incident guided waves.

5 Brief summary

The transmission and reflection coefficients of the two-dimensional semi-infinite solid-solid phononic crystal system and fluid-fluid phononic waveguide structures have been investigated. For the solid-solid system, the transmission spectra of longitudinally and transversally polarized incident waves are different, and the spectra of the transmission and reflection coefficients of the semi-infinite system agree with the band structure very well. The numerical results also show that the semi-infinite system eliminates the Fabry-Perot interference peaks in the spectra which have been well understood in the context of photonic crystals, and more generally optics. Compared with the propagation behavior of the elastic wave incident from the host into phononic crystals and the inverse process, the spectra for these two processes are identical, which means that the original and inverse processes are symmetrical when the time is reversed. For the semi-infinite phononic waveguide, the transmission coefficient is not very high when the frequency is near to the cutoff frequency. This means that the coupling efficiency varies with the frequency of the incident guided mode; far from the cutoff frequency, the guided wave couples out of the waveguide with very high efficiency. Finally, more complicated sandwiched waveguide structures have been investigated. The numerical results show that when the guide wave is incident, the localized mode will be excited, and a different polarity has different coupling efficiency with the incident guided wave.

This work was supported by the National Natural Science foundation of China under Grant No. 10674032 and Guangdong Provincial Natural Science Foundation of China under Grant No. 013009.

References

1. L.M. Brekhovskikh, *Waves in Layered Media* (Academic New York, 1960)
2. R.E. Camley, B. Djafari-Rouhani, L. Dobrzynski, A.A. Maradudin, Phys. Rev. B **27**, 7318 (1982)
3. B. Djafari-Rouhani, L. Dobrzynski, O. Hardouin Duparc, R.E. Camley, A.A. Maradudin, Phys. Rev. B **28**, 1711 (1983)
4. M.S. Kushwaha, Appl. Phys. Lett. **70**, 3218 (1997)
5. Fugen Wu, Zhengyou Liu, Youyan Liu, Phys. Rev. E **66**, 046628 (2002)
6. Zhengyou Liu, C.T. Chan, Ping Sheng, A.L. Goertzen, J.H. Page, Phys. Rev. B **62**, 2446 (2000)
7. I.E. Psarobas, N. Stefanou, A. Modinos, Phys. Rev. B **62**, 278 (2000)
8. L. Sanchis, A. Hákansson, F. Cervera, J. Sánchez-Dehesa, Phys. Rev. B **67**, 035422 (2003)
9. C. Goffaux, J. Sánchez-Dehesa, Phys. Rev. B **67**, 144301 (2003)
10. D. Caballero, J. Sánchez-Dehesa, C. Rubio, R. Mártinez-Sala, J.V. Sánchez-Pérez, F. Meseguer, J. Llinares, Phys. Rev. E **60**, R6316 (1999)
11. Yukihiro Tanaka, Yoshinobu Tomoyasu, Shin-ichiro Tamura, Phys. Rev. B **62**, 7387 (2000)
12. C. Goffaux, J.P. Vigneron, Phys. Rev. B **64**, 075118 (2001)
13. J.O. Vasseur, P.A. Deymier, B. Chenni, B. Djafari-Rouhani, L. Dobrzynski, D. Prevost, Phys. Rev. Lett. **86**, 3012 (2001)
14. J.O. Vasseur, P.A. Deymier, A. Khelif, Ph. Lambin, B. Djafari-Rouhani, A. Akjouj, L. Dobrzynski, N. Fettouhi, J. Zemmouri, Phys. Rev. E **65**, 056608 (2002)
15. D. García-Pablos, M. Sigalas, F.R. Montero de Espinosa, M. Torres, M. Kafesaki, N. García, Phys. Rev. Lett. **84**, 4349 (2000)
16. M. Torres, F.R. Montero de Espinosa, D. García-Pablos, N. Garcia, Phys. Rev. Lett. **82**, 3054 (1999)
17. A. Khelif, B. Djafari-Rouhani, J.O. Vasseur, P.A. Deymier, Phys. Rev. B **68**, 024302 (2003)
18. A. Khelif, A. Choujaa, S. Benchabane, Appl. Phys. Lett. **84**, 4400 (2004)
19. M.M. Sigalas, J. Acoust. Soc. Am. **101**, 1256 (1997)
20. M. Kafesaki, M.M. Sigalas, N. García, Phys. Rev. Lett. **85**, 4044 (2000)
21. Xiangdong Zhang, Zhengyou Liu, Appl. Phys. Lett. **85**, 341 (2004)
22. Yongjun Cao, Zhilin Hou, Wichit Sritrakool, Youyan Liu, Phys. Lett. A **337**, 147 (2005)
23. Zhilin Hou, Fugen Wu, Xiujun Fu, Youyan Liu, Phys. Rev. E **71**, 037604 (2005)
24. Tsung-Tsong Wu, Zin-Chen Hsu, Zi-Gui Huang, Phys. Rev. B **71**, 064303 (2005)
25. Yukihiro Tanaka, Shin-ichiro Tamura, Phys. Rev. B **58**, 7958 (1998)
26. Zhilin Hou, Xiujun Fu, Youyan Liu, Phys. Rev. B **70**, 014304 (2004)
27. Yuanwei Yao, Zhilin Hou, Youyan Liu, Physica B **388**, 75 (2007)
28. Zhiyuan Li, Kaiming Ho, Phys. Rev. B **68**, 155101 (2003)
29. L.C. Botten, N.A. Nicorovici, R.C. McPhedran, C. Martijn de Sterke, A.A. Asatryan, Phys. Rev. E **64**, 046603 (2001)
30. L.C. Botten, T.P. White, A.A. Asatryan, T.N. Langtry, C. Martijn de Sterke, R.C. McPhedran, Phys. Rev. E **70**, 056606 (2004)
31. S. Mingaleev, K. Busch, Opt. Lett. **28**, 619 (2003)
32. Xiaochun Li, Zhengyou Liu, Solid State Commun. **133**, 397 (2005)